



Journal of Materials and Engineering Structures

Research Paper

Structural characteristics of simply connected planar sections with application to airfoils

Zebbiche Toufik ^{a,*}, Boun-jad Mohamed ^a, Allali Abderrazak ^b

^aAeronautical Science Laboratory, Institute of Aeronautics and Space Studies, University of Blida 1, Algeria

^bAircraft Laboratory, Institute of Aeronautics and Space Studies, University of Blida 1, Algeria

ARTICLE INFO

Article history :

Received : 7 April 2014

Revised : 29 July 2014

Accepted : 7 August 2014

Keywords:

Triangular element

Simply connected domain

Airfoil

Cubic spline interpolation

ABSTRACT

The presented work is to develop a numerical computation program to determine the geometrical characteristics of arbitrary simply connected planar sections and applications to airfoils. In the literature, there are exact analytical solutions only for some simples' geometries, such as circular, rectangular and elliptical sections. Hence our interest is focused on the search of approximate numerical solutions for more complex sections used in aeronautics. The used method is to subdivide the section in the infinitesimal triangular sections with a single observer within the area having a suitable position. The characteristics of any triangle, given by the positions of these three nodes are known in the literature. Using the principle of compound surfaces, one can determine the geometric characteristics of the airfoil surface. The analytic function of the airfoil boundary is obtained by using the cubic spline interpolation because the airfoil is given in the form of tabulated points. Error estimation is done to determine the accuracy of the numerical computation.

1 Introduction

The geometric characteristics of a section, in particular for geometry of an airfoil play a very important role for the calculation of strength of materials or elasticity for example. By external stress applied, the calculation of the stress distribution is related to the knowledge of the geometric characteristics of the section of the structure [1], [2] and [3]. Such buckling beams occur about the axis having the moment of inertia as small as possible. So the critical buckling force is related to the small value of the moment of inertia. Hence our interest is directed towards the calculation of moment of inertia I_{min} . In addition, the second example is the phenomenon of torque. So, the torsional stress is related to the knowledge of the value of polar moment of inertia I_p . In the general case of circular cross-sections are used. But for a plane, most of the structures are non-circular [4]. Hence our interest is also aimed for calculating the polar inertia moment of airfoils.

* Corresponding author. Tel.: +213 (0)662197226.

E-mail address: z_toufik270169@yahoo.fr

Another important phenomenon is the determination of the distribution of the bending stress that is simple or deflected. This constraint is related to the both inertia moments along the two axes of applications of bending moment and the product of inertia of the considered section. The calculation of these moments of inertia must be done to respect to axes through the center of gravity of the section. So in this case it is necessary to determine the position of the center of gravity of the section relative to the mark definition of the field.

This study is then to produce a program for numerical computation of geometrical properties of plane simply connected complex sections and make the application to airfoils using the principle of the discretization of the domain into triangular elements with one observer inside the area, provided that all nodes of the domain boundary is visible by the internal point (observer). The triangles are defined by the positions of these three nodes [5]. Two nodes are on the boundary and the third one is that the internal point. The geometric characteristics of any triangle are known [5], [6], [7], [8] and [9]. Using the principle of the composite surface, it may determine the geometric characteristics of this surface. As the number of triangle is very important, the calculation becomes numerical. The accuracy of the calculation depends on the discretization. More the number of triangles is high, more we have a good accuracy. Generally, the boundary of the airfoil is given in the form of tabulated points [4]. Then the points must be interpolated to determine an analytical form of the geometry. The choice is the cubic spline interpolation [10] and [11]. This is a very good interpolation. It keeps the curvature of the airfoil at the leading edge. Our application is limited for airfoils used in subsonic and transonic regime of flight.

2 Geometric characteristics of a triangle

The triangular element is presented by the boundary nodes as presented in figure 1. The coordinates of nodes 1, 2, 3 are known in relation to any reference xoy.

The geometric characteristics A , x_G , y_G , S_x , S_y , I_x , I_y and I_{xy} can be determined by the following integral with $m=0, 1, 2$ and $n=0, 1, 2$ [5], [7], [8] and [9] :

$$I_{mn} = \int_{\Delta} x^m y^n dx dy \quad (m=0, 1, 2) \quad (n=0, 1, 2) \quad (1)$$

Then $A=I_{00}$, $S_x=I_{01}$, $S_y=I_{10}$, $I_{xx}=I_{02}$, $I_{yy}=I_{20}$ and $I_{xy}=I_{11}$. Using these relations, we can calculate the geometric characteristics and the position x_G , y_G of the center of gravity of a triangular surface with respect to any axis as follows.

$$A = \frac{1}{2} [x_1(y_2 - y_3) + x_2(y_3 - y_1) + x_3(y_1 - y_2)] \quad (2)$$

$$x_G = \frac{1}{3} (x_1 + x_2 + x_3) \quad (3)$$

$$y_G = \frac{1}{3} (y_1 + y_2 + y_3) \quad (4)$$

$$S_x = A y_G \quad (5)$$

$$S_y = A x_G \quad (6)$$

$$I_y = \frac{A}{12} [x_1^2 + x_2^2 + x_3^2 + 9 x_G^2] \quad (7)$$

$$I_x = \frac{A}{12} [y_1^2 + y_2^2 + y_3^2 + 9 y_G^2] \quad (8)$$

$$I_{xy} = \frac{A}{12} [x_1 y_1 + x_2 y_2 + x_3 y_3 + 9 x_G y_G] \quad (9)$$

The numbering of the nodes must be made in the counterclockwise direction.

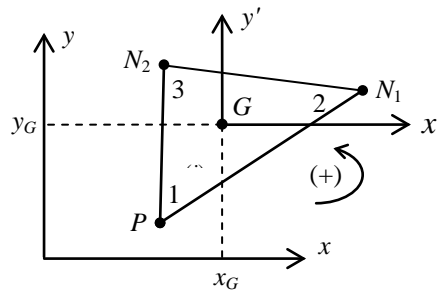


Fig. 1 - Triangular element with three-nodes.

3 Mesh Generation

It should be noted that the geometry of the airfoil is given in the form of tabulated values [4]. So we used the cubic spline interpolation to find an analytical equation for the upper and lower surface. The number of points selected for the mesh generation is different from that given for the definition of the geometry of the airfoil. We are interested in simply connected domains with a single observer.

3.1 Stretching function

Due to the curvature of the boundary, it is sometimes useful to condense the nodes into a well specified to have a good presentation of the boundary, especially at the leading edge of the airfoil for subsonic wings region.

If the stretching function is applied to the EA side (see Figure 2), for example the airfoil chord, standardized independent variable is given by:

$$\eta^* = \frac{\eta - \eta_A}{\eta_E - \eta_A} \quad (10)$$

with : $0 \leq \eta^* \leq 1$ and $\eta_A \leq \eta \leq \eta_E$

where : η represents x

The stretching function used is given by [5] and [12] :

$$s = P \eta^* + (1 - P) \left[1 - \frac{\tanh [Q(1 - \eta^*)]}{\tanh [Q]} \right] \quad (11)$$

Once the value of s is obtained, it is required to specify the distribution of x . For example

$$x = x_A + s (x_E - x_A) \quad (12)$$

For values of $P > 1.0$, it is possible to condense the nodes to point A .

Typical distributions of points on the EA segment for different values of P and Q , are shown in the following figure 2:

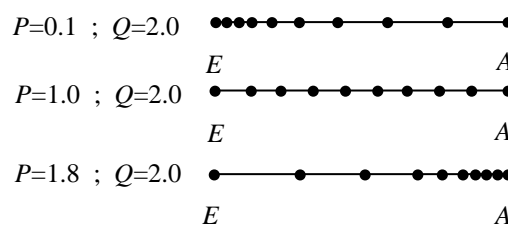


Fig. 2- Distribution of nodes according to equation (12)

Obtained for the ordinate of the considered point on the boundary, it is sufficient to use the analytic function of the upper or lower surface.

3.2 Internal Mesh

The resulting mesh is formed by triangular cells, two nodes of each triangle are on the boundary of the airfoil and the third node is located in the inner surface of the airfoil. The internal point is common to all the triangles formed in the domain. The position of internal node must be chosen so that it is *visible* to all nodes of the boundary. If for example the node is not visible to some points of the boundary, we must in this case to change the position of the internal node as the first solution, or to divide the area of airfoil by several blocks. For each block we must choose the internal point so that it is visible to all nodes in the block. For our chosen geometry of airfoils, the resolution of this problem is by changing the internal point; see Figure 3, 4, 5, 6 and 7.

3.3 Connecting triangles in a mesh

The numbering of the nodes of the mesh starts with the trailing edge counter clockwise. Then the internal point is appointed by the point P outside dialling. If the number of points on the boundary is NN , then the total number of points is one $NN+1$. Therefore the number of treated triangle is equal to $NT = NN$.

The problem is to assemble these triangles to get the result for the entire domain. To get results, we must have to know the numbers of nodes of each triangle, see Figure 1. For the triangle number (i) ($i = 1, 2, 3, \dots, NT$), the nodes N_1 and N_2 respectively takes the values i and $i+1$. For the last triangle, the number of node $N_2 = 1$ (closure of the boundary). For this triangle, one side is on the lower side with a node that is the trailing edge.

4 Geometric characteristics of the composite section (Airfoil)

Surface area has been divided into small triangular elements. Then, the calculation of geometrical characteristics for the entire domain is approximated by the sum of all the geometric characteristics of triangles constituting the field. So we can write:

$$A = \sum_{i=1}^{i=NT} A_i \quad (13)$$

$$S_x = \sum_{i=1}^{i=NT} (y_G)_i A_i \quad (14)$$

$$S_y = \sum_{i=1}^{i=NT} (x_G)_i A_i \quad (15)$$

$$I_x = \sum_{i=1}^{i=NT} (I_x)_i \quad (16)$$

$$I_y = \sum_{i=1}^{i=NT} (I_y)_i \quad (17)$$

$$I_{xy} = \sum_{i=1}^{i=NT} (I_{xy})_i \quad (18)$$

The center of gravity of this section is given by the equations (5) and (6).

The terms under the summation sign in the relations (13), (14), (15), (16), (17) and (18) are given by the relations in a triangle, presented by the relations (2), (5), (6), (7), (8) and (9).

The geometric characteristics of the entire section from the central axis can be determined by using the Hugues theorem (parallel axis theorem) [1], [2] and [3]. So we have:

$$I'_x = I_x - y_G^2 A \quad (19)$$

$$I'_y = I_y - x_G^2 A \quad (20)$$

$$I'_{xy} = I_{xy} - x_G y_G A \quad (21)$$

The polar moment of inertia of the entire section can be calculated by the following equation [5]. Then:

$$I_p = I'_x + I'_y \quad (22)$$

Can be determined as a result, the two values of principal moments of inertia and the principal directions by simple relationships known in the literature [1], [2] and [3]. The key to these results is the central inertia moment given by the relations (19), (20) and (21).

To justify the accuracy of the obtained results, it is recommended to calculate the error of the numerical calculation and accurate results. The exact solution for the airfoils results do not exist. We can choose a simple section, like half circle, and discretize it with the same approach presented and see the convergence of the solution in terms of number of nodes. All this must be done by the same developed numerical calculation program. Then, for each parameter A , x_G , y_G , I'_x , I'_y , I'_{xy} , the value of the relative error may be computed by the following formula:

$$\varepsilon \% = \frac{\left| \text{Parameter}_{\text{Computed}} - \text{Parameter}_{\text{exact}} \right|}{\text{Parameter}_{\text{exact}}} \times 100 \quad (23)$$

5 Results and comments

In Figures 3, 4, 5, 6 and 7 were taken the following parameters $P=1.90$, $Q=2.00$ for the extrados and $P=0.01$, $Q=2.00$ for intrados. Note that the numbering of the nodes on the upper surface begins from the trailing edge to the leading edge whereas for the lower surface, the numbering of nodes starts from the leading edge to the trailing edge. The mesh is made so that there is condensation of nodes to the edge for rounding the bend. This procedure is especially important for subsonic and transonic airfoils.

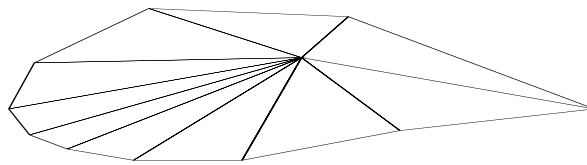


Fig. 3 - Triangular mesh on the surface of a wing airfoil with NT=10.

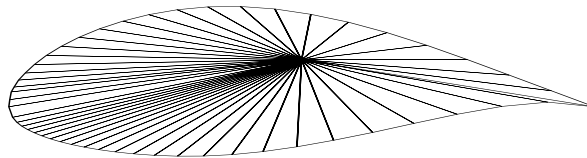


Fig. 4 - Triangular mesh on the surface of a wing airfoil with NT=50.

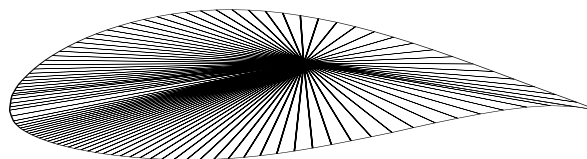


Fig. 5 - Triangular mesh on the surface of a wing airfoil with NT=100.

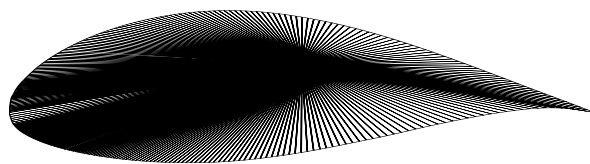


Fig. 6 - Triangular mesh on the surface of a wing airfoil with $NT=300$.

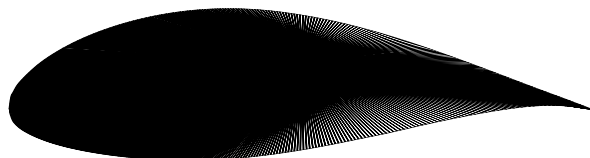


Fig. 7 - Triangular mesh on the surface of a wing airfoil with $NT=600$.

For example, for the following figure 8, the inside point P is not *visible* in the last two segments of the lower surface adjacent to the trailing edge, while this configuration is no longer valid for the calculation of geometric characteristics.

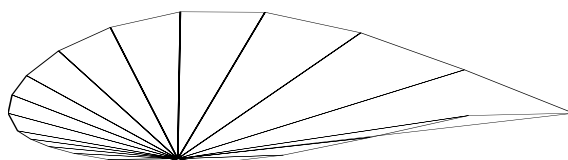


Fig. 8 - Position of internal point where it is no longer visible to the last segment of the lower surface.

In Figures 3, 4, 5, 6 and 7, the scale is not chosen orthonormal in order to see the distribution of nodes on the boundary.

The airfoil selected from these figures is that the non-symmetrical NACA 63-412 with camber. The points defining the geometry are shown in Table 1. Note that this airfoil is presented by 26 points on each side. The data points in the airfoil presented in Table 3 can be found in references [4]. The points of the table 1 are used to determine the analytical function of the extrados and the intrados of using cubic spline interpolation.

Table 1 – Definition of the NACA 63-412 airfoil surface

Upper surface in (%) of C						Lower surface in (%) of C					
	x/C (%)	y/C (%)		x/C (%)	y/C (%)		x/C (%)	y/C (%)		x/C (%)	y/C (%)
1	0.000	0.000	14	39.924	8.062	1	0.000	0.000	14	40.076	-3.778
2	0.336	1.071	15	44.964	7.894	2	0.664	-0.871	15	45.035	-3.514
3	0.567	1.320	16	50.000	7.567	3	0.933	-1.040	16	50.000	-3.164
4	1.041	1.719	17	55.031	7.125	4	1.459	-1.291	17	54.969	-2.745
5	2.257	2.460	18	60.057	6.562	5	2.743	-1.716	18	59.943	-2.278
6	4.727	3.544	19	5.076	5.899	6	5.273	-2.280	19	64.924	-1.799
7	7.218	4.379	20	70.087	5.153	7	7.782	-2.685	20	69.913	-1.265
8	9.718	5.063	21	75.089	4.344	8	10.282	-2.995	21	74.911	-0.764
9	14.735	6.138	22	80.084	3.492	9	15.265	-3.446	22	79.916	-0.308
10	19.765	6.929	23	85.070	2.618	10	20.235	-3.745	23	84.930	0.074
11	24.800	7.499	24	90.049	1.739	11	25.200	-3.919	24	89.951	0.329
12	29.840	7.872	25	95.023	0.881	12	30.160	-3.984	25	94.977	0.330
13	34.882	8.059	26	100.000	0.000	13	35.111	-3.939	26	100.000	0.000

The second problem is to justify the convergence of the numerical results to the exact solution. Taking the example of a half-circle of radius $R=1.00$ placed at the origin of coordinates. It is only interested in the convergence of values A , y_G , I_x' , I_y' and I_{xy}' since they depend on the discretization. In that case $x_G=0.0$ and $I_{xy}'=0.00$ for reasons of symmetry. We can deduce the other parameters such as I_{max} and I_{min} and the orientation of the principal axes of inertia, through the application of analytical relationships [1], [2] and [3]. Results on the cross-sectional area are normalized by the square of the value of the section chord. About the center of gravity, it is normalized by the chord of the airfoil. For the moments of inertia, the results are normalized by C^4 . The search results are presented in Table 2.

Table 2 - Effect of discretization on the convergence

NT	A/C^2	y_G/C	I_x'/C^4	I_y'/C^4
10	1.366025	0.410683	0.095860	0.273424
50	1.556667	0.425612	0.108811	0.380670
100	1.565860	0.425038	0.109356	0.388254
200	1.569144	0.424676	0.109594	0.391161
500	1.570370	0.424495	0.109706	0.392290
1000	1.570705	0.424431	0.109745	0.392612
3000	1.570793	0.424414	0.109755	0.392696
7000	1.570802	0.424413	0.109756	0.392704

We note from the table 2, the cross-sectional area converges to the exact section before the convergence of y_G then I_x' and I_y' . To have an accuracy of $\epsilon=10^{-6}$, it takes about a discretization of 7000 points for this section.

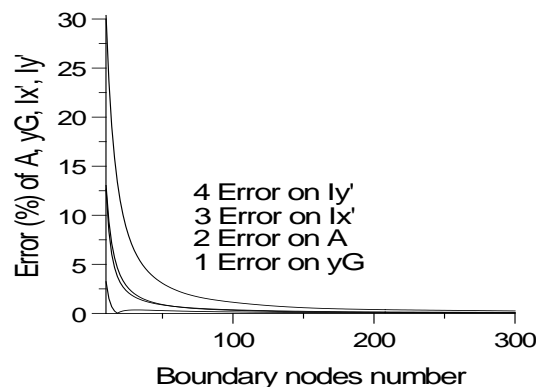


Fig. 9 - Relative error parameters A , y_G , I_x' and I_y' according to the number of points of the boundary

The figure 9 shows the relative error on the parameters A , y_G , I_x' and I_y' according to the number of points on the domain boundary. Note that the convergence is made of monotonically way. We still notice that the value of y_G converge first then the cross-sectional area, moment of inertia then central I_x' and ending the central inertia I_y' .

The values in tables 3, 4 and 5 are obtained for a discretization of 7000 points on the domain boundary.

According to table 5, we see that the moment of inertia I_x' is much lower than the moment of inertia I_y' , because the size of the airfoil thickness is much smaller than the chord of the airfoil.

Determining the centroid position is made relative to the reference of the definition section. This marker is associated with the leading edge of the section (airfoil).

The airfoils selected in this publication regarding all airlines. It took 32 airfoils as this table 3 shows them.

Table 3 - Area of several airfoils geometries

N°	Airfoil	A/C^2	N°	Airfoil	A/C^2
1	NACA0012	0.082055	17	NACA M1	0.043951
2	NACA 63-412	0.075572	18	ONERA OA209	0.063816
3	RAE 2822	0.077874	19	OAF 128	0.077549
4	NACA 0010-34	0.070332	20	ONERA NACA CAMBRE	0.078835
5	NACA 62	0.079999	21	NASA LANGLEY RC-08 B3	0.058713
6	RAF 30	0.084460	22	NASA LANGLEY RC-08 N1	0.052830
7	E-385	0.052908	23	TRAINER 60	0.117166
8	NACA 23009	0.061020	24	TSAGI 8%	0.055092
9	NACA 2412	0.081935	25	TSAGI 12%	0.082490
10	NASA AMES A-01	0.073867	26	EPPLER 520	0.096675
11	AQUILA 9.3%	0.062041	27	EPPLER 635	0.076116
12	AVISTAR	0.098823	28	LOCKHEED L-188 ROOT	0.096874
13	CHEN	0.080130	29	NACA 63-415	0.093841
14	FAUVEL 14%	0.088348	30	NACA 63-210	0.063168
15	EIFFEL 385	0.085813	31	NACA 64-108	0.050974
16	WORTMANN FX 2	0.135732	32	NASA LANGLEY 64-012	0.075871

Table 4 - Position of centroid for various airfoils.

N°	x_G/C	y_G/C	N°	x_G/C	y_G/C
1	0.420140	0.000000	17	0.435090	0.000000
2	0.408059	0.018247	18	0.422121	0.010153
3	0.423024	0.004443	19	0.380560	0.007638
4	0.456492	0.010800	20	0.424568	0.009142
5	0.424989	0.000000	21	0.448388	0.007719
6	0.417490	0.000000	22	0.429594	0.011036
7	0.395866	0.065633	23	0.402856	0.001122
8	0.416665	0.012368	24	0.434106	0.008528
9	0.420004	0.015671	25	0.434231	0.012695
10	0.427888	0.010394	26	0.411404	0.000000
11	0.412244	0.031870	27	0.412580	0.015713
12	0.431799	0.016442	28	0.433125	0.015941
13	0.406882	0.047129	29	0.406008	0.018335
14	0.391245	0.013107	30	0.409342	0.009139
15	0.396116	0.063444	31	0.417749	0.004563
16	0.448082	0.025545	32	0.415146	0.000000

Airfoils that have $y_G=0.0$ mean that this airfoil is symmetrical. In this case the product of inertia $I_{xy}'=0.0$. These results are found for the airfoil number 1 (NACA 0012), number 5 (NACA 62), number (RAF 30) and number 17 (NACA M1) from Table 3.

To study the phenomenon of tension and compression of the blades of compressors and turbines, we are interested to know the area of the section as presented Table 3.

The results presented in table 5 are very interesting to study the bending the blades of compressors and turbines and other possible configurations. The polar moment of inertia is aimed to study the phenomenon of torsion of wing airfoil.

Table 5 - Central moments and the polar moment of inertia for different airfoils.

N°	$I_x'/C^4 \times 10^4$	$I_y'/C^4 \times 10^2$	$I_{xy}'/C^4 \times 10^4$	$I_p/C^4 \times 10^2$
1	0.680850	0.449961	0.000000	0.456769
2	0.626664	0.356460	0.333899	0.362727
3	0.656618	0.381017	0.734876	0.387583
4	0.419910	0.381014	0.091848	0.385213
5	0.658346	0.426943	0.000000	0.433526
6	0.776864	0.442631	0.000000	0.450399
7	0.293604	0.256252	0.419879	0.259188
8	0.298304	0.328142	-0.532930	0.331125
9	0.698550	0.446935	0.075475	0.453920
10	0.485877	0.415784	-0.473303	0.420643
11	0.362594	0.323438	-0.483433	0.327064
12	1.213518	0.538859	-0.189258	0.550994
13	1.073318	0.467305	-2.989970	0.478039
14	1.063061	0.453687	-1.845268	0.464318
15	1.003570	0.457915	-1.491523	0.467951
16	3.391618	0.664142	1.998717	0.698059
17	0.098507	0.251254	0.000000	0.252239
18	0.328390	0.343620	-0.512950	0.346904
19	0.683397	0.398350	0.093947	0.405183
20	0.608441	0.432101	-0.551573	0.438186
21	0.235030	0.335478	-0.260739	0.337829
22	0.203703	0.270996	-0.429491	0.273033
23	2.165327	0.618330	-0.163497	0.639983
24	0.214209	0.299568	-0.365493	0.301710
25	0.717247	0.449155	-0.819278	0.456327
26	1.271488	2.093213	0.000000	0.469655
27	0.668562	0.405830	-1.731414	0.412515
28	1.126240	0.521983	0.323426	0.533246
29	1.202264	0.438758	0.408098	0.450780
30	0.358821	0.299137	0.146401	0.302725
31	0.183599	0.244406	0.054539	0.246242
32	0.610931	0.360474	0.000000	0.366583

6 Conclusion

This work allows us to determine the geometrical characteristics of simply connected complex sections used in aeronautics for the study of problems of elasticity. The discretization is made with triangular cells. One point is chosen in the inner area. The problems of elasticity as traction, simple bending or deflected, buckling and twisting can be studied if we know the geometric characteristics of the studied sections. All considered wings airfoil are presented in tabulated values. Since, cubic spline interpolation is used in this case to obtain an analytic function for the upper and lower surface. The airfoils studied involving only the field of incompressible and compressible subsonic and transonic area. The discretization of the domain can be done with any number of triangles. Application is made for a discretization of 7000 triangles. Condensation nodes to the leading edge of the airfoil are used to refine the points to the edge having the large curvature in this region. The central moment of inertia I_y' is much less than I_x' having the dimension of the airfoil thickness (vertical axis) is less than the chord of the airfoil (dimension along the horizontal axis).

Acknowledgements

The authors acknowledge Khaoula, AbdelGhani Amine and Ritadj Zebbiche and Mouza Ouahiba for granting time to prepare this manuscript.

Appendix A. Nomenclature

(x_j, y_j)	Coordinates of a node
NT	Number of triangles in the domain
NN	Number of nodes on the boundary
I_{20}, I_{02}	Moments of inertia of a triangle
I_{10}, I_{01}	Static inertia of a triangle
I_{11}	Product of inertia of a triangle
A, I_{00}	Surface area of a triangle and the airfoil
x_G, y_G	Centred coordinates
I_P	Polar moment of inertia
η^*	Normalized variable
P, Q	Parameters for the control of mesh points (Function of condensation)
C	Chord of an airfoil
I_x', I_y'	Central moments of inertia
I_{xy}'	Central product inertia
P	Internal point of the airfoil
E	Tolerance

REFERENCES

- [1]- I. Miropoliubov, Résistance des matériaux, manuel de résolution de problèmes, 4th Edition, Ed. Mir Moscou, 1977.
- [2]- B.B. Muvdi, J.W. McNabb, Engineering Mechanics of Materials, Macmillan Publishing Company, 1980.
- [3]- G. Pissarenko, A. Yakovlev, V. Matveev, M. Segasayo, Aide mémoire de résistance des matériaux, Ed. Mir Moscou, 1979.
- [4]- I.H. Abbott, A.E. Von Doenhoff, Theory of wing sections: Including a summary of Airfoil data, Dover Publications, Inc., New York, 1959.
- [5]- M. Boun-jad, T. Zebbiche, Résolution de l'équation de Poisson dans un domaine simplement connexe, Editions Universitaire Européenne, 2012, ISBN 978- 3-8417-9282-2.
- [6]- J.-F. Imbert, Analyse des Structures par Eléments Finis, 3rd Edition, Ed. Cépaduès, 1995.
- [7]- H. Kardestuncer, Finite Element Handbook, Ed. McGraw-Hill Book Company, 2010.
- [8]- J.N. Reddy, An Introduction to the Finite Element Method, Ed. Mc-Graw Hill Book Company, 2005.
- [9]- D. Gouri, G. Touzot, Une présentation de la méthode des éléments finis, Ed. Presses Université Laval, 1981.
- [10]- B.P. Demidovitch, I.A. Maron, v. Polonski, Eléments de Calcul Numérique, 2nd edition, Ed. Mir Moscou, 1987.
- [11]- A. Ralston, P. Rabinowitz, A First Course in Numerical Analysis, Dover Publications Inc., 2003
- [12]- C.A.J. Fletcher, Computational Techniques for Fluid Dynamics, Volume II, Specific Techniques for Different Flow Categories, Springer-Verlag, 1988.